

Title: Escalating combinations of enhanced infectivity and immune escape define SARS-CoV-2 Omicron lineage replacement

Authors: Nicholas F.G. Chen¹, Kien Pham¹, Chrispin Chaguza^{1,2}, Rafael Lopes^{1,2}, Fayette Klaassen³, Daniel M. Weinberger^{1,2}, Virginia E. Pitzer^{1,2}, Joshua L. Warren^{2,4}, Nathan D. Grubaugh^{1,2,5*}, Anne M. Hahn^{1*,#}

¹ Department of Epidemiology of Microbial Diseases, Yale School of Public Health, New Haven, United States,

² Public Health Modeling Unit, Yale School of Public Health, New Haven, United States,

³ Department of Global Health & Population, Harvard T. H. Chan School of Public Health, Boston, United States,

⁴ Department of Biostatistics, Yale School of Public Health, New Haven, United States

⁵ Department of Ecology and Evolutionary Biology, Yale University, New Haven, United States

* These authors contributed equally to this work.

corresponding author: anne.hahn@yale.edu

Abstract: In 2022, consecutive sweeps of the highly transmissible SARS-CoV-2 Omicron-family maintained high viral transmission levels despite extensive antigen exposure on the population level resulting from both vaccinations and infections. To better understand variant fitness in the context of the highly dynamic immunity landscape of 2022, we aimed to dissect the interplay between immunity and fitness advantages of emerging SARS-CoV-2 Omicron lineages on the population-level. We evaluated the relative contribution of higher intrinsic transmissibility or immune escape on the fitness of emerging lineages by analyzing data collected through our local genomic surveillance program from Connecticut, USA. We compared growth rates, estimated infections, effective reproductive rates, average viral copy numbers, and likelihood for causing vaccine break-through infections.

Using these population-level data, we find that newly emerging Omicron lineages reach dominance through a specific combination of enhanced intrinsic transmissibility and immune escape that varies over time depending on the state of the host-population. Using similar frameworks that integrate whole genome sequencing together with clinical, laboratory, and epidemiological data can advance our knowledge on host-pathogen dynamics in the post-emergence phase that can be applied to other communicable diseases beyond SARS-CoV-2.

NOTE: This preprint reports new research that has not been certified by peer review and should not be used to guide clinical practice.

1 **Main Text**

2 **Introduction**

3 Capacities for genomic surveillance saw an unprecedented rise during the COVID-19 pandemic (Brito
4 et al. 2022). The ability to closely monitor SARS-CoV-2 populations in real-time was crucial to discover
5 and track SARS-CoV-2 variants of concern (VOC). The first VOC, Alpha (B.1.1.7) (Hill et al. 2022;
6 Rambaut et al. 2020), emerged towards the end of 2020 and was followed in 2021 by Beta (B.1.351)
7 (Tegally et al. 2021), Gamma (P.1) (Faria et al. 2021), and Delta (B.1.617) (WHO 2021). In late 2021,
8 the highly divergent Omicron (B.1.1.529) lineage (Viana et al. 2022) rapidly displaced Delta globally.

9 In 2022, SARS-CoV-2 transmission remained, somewhat counterintuitively, high all year, which stands
10 in contrast to the summer-lows observed during 2020 and 2021. This was characterized by consecutive
11 sweeps of multiple Omicron lineages. BA.1 (B.1.1.529.1), the first member of the Omicron family to
12 emerge, shared a common ancestor with the D614G background in late 2020. This ancestor diverged
13 into at least five main sublineages (BA.1-BA.5) (Tegally et al. 2022; Viana et al. 2022). The exact origin
14 and nature of the emergence of these Omicron lineages remains unclear; however, it is likely that these
15 lineages emerged from a common source, likely undergoing selective pressure for an extended amount
16 of time (Markov et al. 2023). A subset of the original Omicron viral population further spread in one or
17 multiple transmission events to a larger community and eventually worldwide (Tegally et al. 2023).

18 Thus, 2022 saw a unique combination of this highly divergent virus variant facing a host population
19 that, through intensive vaccination campaigns and vaccine roll-out in many parts of the world, had built
20 up significant amounts of immunity towards the original Wuhan-Hu-1 Spike antigen. In this study, we
21 aimed to reconstruct key epidemiological and evolutionary features that led to the particular lineage
22 replacement dynamics of Omicron lineages as exemplified in a well-monitored study setting in
23 Connecticut, United States (US). For this, we drew upon sample data collected from the Yale New

24 Haven Hospital (YNHH) through our Yale Genomic Surveillance Initiative from January 2022 to
25 January 2023. Whole genome sequencing data together with relevant laboratory and patient metadata
26 were available for approximately 5-10% of total reported cases across the state and the entire length of
27 the study period. To characterize competitive growth advantages of variants during their emergence
28 periods and evaluate their fitness compared to their immediate predecessors, we calculated the growth
29 rates of each incoming Omicron lineage, compared their virus copy number from nasal swabs, and
30 calculated the risk for vaccine breakthrough infections as a metric for immune escape. Doing so, we
31 reveal a high capacity of Omicron lineages to explore different fitness niches through a combination of
32 enhanced transmissibility and/or immune escape depending on the history of antigenic exposure of the
33 host-population.

34 The synthesis of high-resolution epidemiological, genomic, and immunological data allows us to assess
35 and compare transmissibility and immune escape of each Omicron lineage. Exploring lineage
36 replacement dynamics on a population level allows us to evaluate predictions based on *in-vitro* data and
37 thus evaluate key parameters defining future variant emergence. Doing so, we reveal a high capacity of
38 Omicron lineages to explore different fitness niches through a combination of enhanced transmissibility
39 and/or immune escape depending on the history of antigenic exposure of the host-population. Our study
40 highlights the ability to derive key aspects of pathogen lineage fitness by analyzing data that can be
41 drawn from genomic surveillance efforts with relatively simple technical requirements. Such
42 frameworks will be particularly relevant for further monitoring SARS-CoV-2 in the post-pandemic
43 phase and are easily transferable to other pathogens.

44 **Results**

45 **Continuous Omicron lineages replacement causes high levels of community** 46 **transmission throughout 2022**

47 Close monitoring of the SARS-CoV-2 population composition added valuable insights on how
48 emerging variants were impacting COVID-19 case dynamics. The first VOCs detected in Connecticut
49 were Alpha in late 2020 and Delta around mid-2021 (**Fig 1A**, based on data from GISAID for
50 Connecticut). Looking at the epidemic curve in Connecticut (**Fig 1B**), the introduction of both the Alpha
51 and Delta VOCs were followed by a surge in reported SARS-CoV-2 cases in December 2020 and Spring
52 2021, respectively. After a summer of relatively low transmission in 2021, cases started to rise again
53 towards the end of the year with a second Delta-dominated peak in December 2021.

54 Globally, the first Omicron sample was identified in November 2021 and shortly after also detected in
55 the US and Connecticut (**Table 1**). BA.1 is an outgroup to the BA.2/BA.4/BA.5 cluster, and XBB a
56 recombinant of two second generation BA.2 lineages (BA.2.10 & BA.2.75) that likely arose in
57 Southeast-Asia around late summer 2022 (Goh et al. 2023) (**Supplementary Fig 1**). Notably, whereas
58 BA.1-BA.5 most likely originated from a common source (Tegally et al. 2021, 2022; Viana et al. 2022),
59 XBB derived from lineages that emerged through sustained transmission chains in 2022. After BA.1's
60 emergence in Connecticut in November 2021, the rapid replacement of Delta was accompanied by a
61 massive increase in reported cases. Then, BA.2 swiftly replaced BA.1 in March 2022. BA.4 and BA.5
62 were both introduced to Connecticut in May 2022 and co-circulated for eight months until December
63 2022 (**Table 1**). Lastly, XBB-based variants outcompeted BA.5 lineages towards the end of 2022.
64 Interestingly, the New England region including our study site was the first where XBB.1.5 was widely
65 circulated within the US (Ma et al. 2023).

66 *Table 1 Major Omicron lineages in Connecticut January 2022 - January 2023, info taken from GISAID*

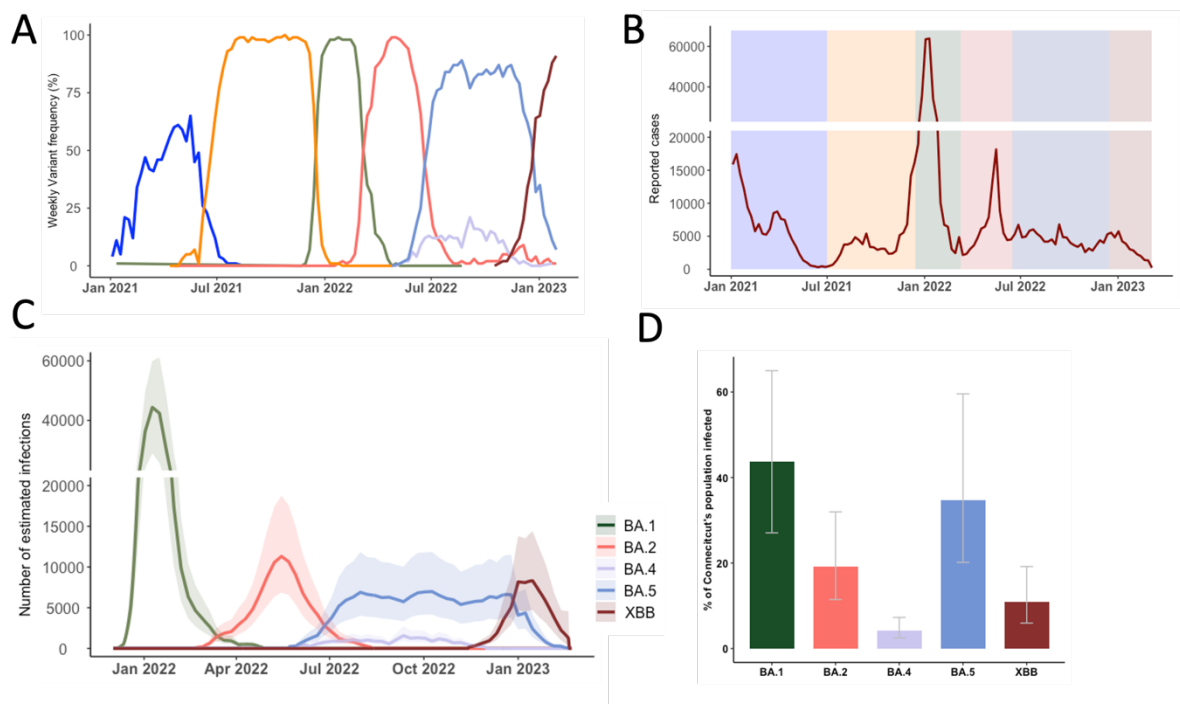
Lineage	First detected globally	First detected in CT	Major sub-lineages in Connecticut (+key amino acid changes in Spike)
BA.1	October 2021	November 2021	BA.1.1 (+R346K)
BA.2	November 2021	January 2022	BA.2.12.1 (+L452Q,S704L)
BA.4	November 2021	May 2022	BA.4.6 (+R346T, N658S)
BA.5	November 2021	May 2022	BQ.1.1 (+R346T, K444T,N460K) BF.7 (+R346T)
XBB (BA.2.10*x BA.2.75*)	September 2022	October 2022	XBB.1.5 (+F486P)

67 To understand the factors that influenced the consecutive sweeps of Omicron lineages, we first
68 characterized the infection dynamics broken up for each lineage with respect to case counts across our
69 one-year study period. As the northern hemisphere entered into the summer months of 2022, most
70 pandemic response mechanisms and non-pharmaceutical measures were discontinued. Consequently,
71 case reporting is expected to be less reliable in accurately mirroring true infection dynamics compared
72 to earlier in the pandemic. Therefore, we retrieved data from covidestim, a Bayesian nowcasting model
73 incorporating publicly available time series of COVID-19 case notifications, hospitalizations, and
74 deaths, accounting for effective population immunity to estimate infections (Chitwood et al. 2022).
75 Together with the frequencies of the major Omicron lineages derived from state-wide genomic
76 surveillance data, we partitioned the overall estimated infections to calculate variant-specific infection
77 estimates cumulatively and over time.

78 By analyzing the variant-specific estimated infections generated through covidestim, we are further able
79 to characterize dynamics of each lineage that may not be reflected in reported cases (**Fig 1C**). Using
80 this framework, we estimated that the BA.1 lineage caused approximately 1.5 million infections in

81 Connecticut, USA (**Fig 1D**), representing around 44% (Credible Interval (CrI) 27%-65%) of the state's
 82 population. Interestingly, the BA.2, BA.4, and BA.5 lineages caused over 2.1 million combined
 83 infections (CrI 1.2-3.5 million) within only nine months after this surge (**Fig 1D**). Another surge driven
 84 by the XBB lineage and its descendants caused an estimated 0.4 million infections (CrI 0.2-0.7 million)
 85 up until January 2023.

86 Taken together, we reconstructed in detail the SARS-CoV-2 infection dynamics caused by Omicron
 87 sublineages in 2022 by drawing upon data from genomic surveillance and epidemiological modeling.
 88 We showed the timing and scale of each of the genetically closely related Omicron lineages differed
 89 substantially and we thus aimed to further characterize each of the emergence periods.



90
 91 **Fig 1. Genomic Epidemiology of SARS-CoV-2 describes the COVID-19 epidemic in Connecticut, US. (A)**
 92 Frequencies of SARS-CoV-2 variants of concern from January 2021 to January 2023, based on sequences deposited on
 93 GISAID. **(B)** Reported COVID-19 infections from January 2021 to 2023 with highlights of the dominant periods of
 94 different Omicron lineages, data from the Connecticut Department of Public Health **(C)** Number of estimated infections
 95 based on the covidestim model for 2022 where testing and reporting widely changed after the first wave of Omicron
 96 BA.1 **(D)** Cumulative estimated cases for each Omicron variant up until January 2023.

97 **Growth advantage of emerging Omicron lineages shrinks towards the end**
98 **of 2022**

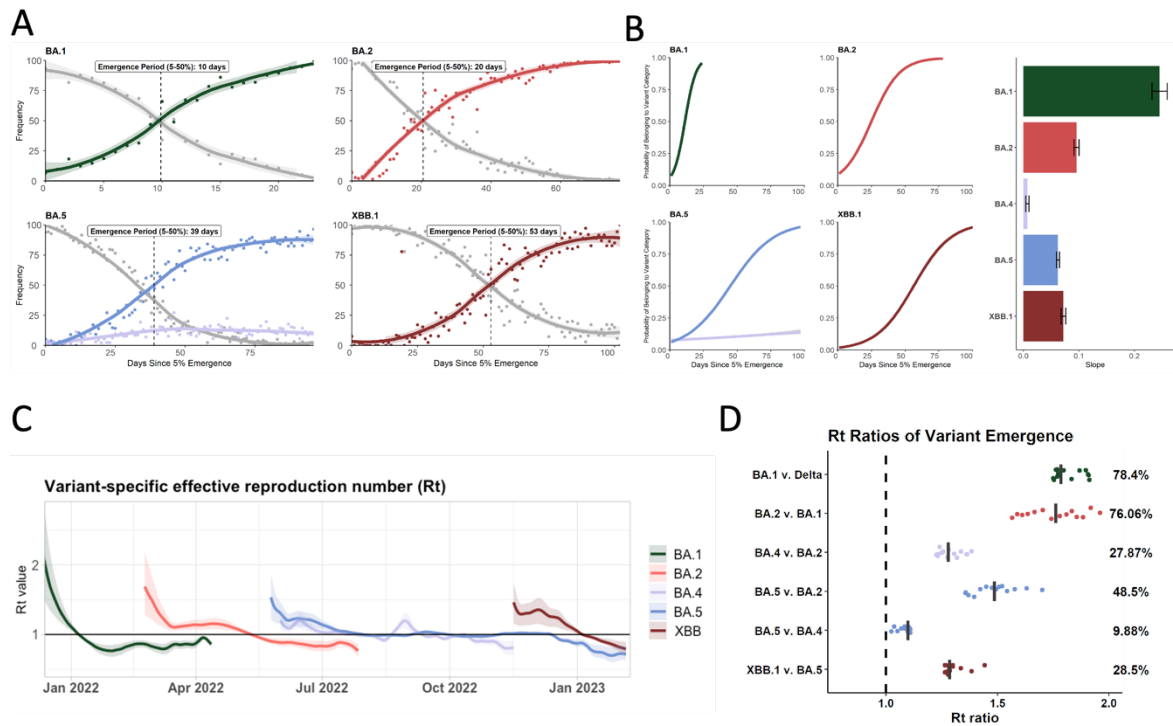
99 Having established that each of these variants exhibits distinct epidemic dynamics in the population,
100 we aimed to further explore the specific features of each of the variants and how these contributed to
101 this emergence pattern. For this, we first determined the rate of lineage replacement by calculating the
102 time it took for each lineage to increase from 5% to 50% of all reported daily cases in Connecticut (Fig
103 2A). This range of 5% to 50% was chosen to capture the period of time it took for a variant to become
104 reliably established in the population, while avoiding some of the inherent stochasticity associated with
105 initial cases, to when it accounted for the majority of cases and is thus dominant in the population. We
106 then fitted a logistic regression model to the observed frequencies and compared their slope coefficients
107 **(Fig 2B)**.

108 Doing so, we show that BA.1 had the fastest growth rate, reaching a frequency of 50% in only 10 days
109 from being detected at 5% **(Fig 2A)**. For each of the subsequent lineages, lineage replacement slowed
110 down, ranging from 20 to 59 days for BA.2 and XBB, respectively.

111 We further compared the emergence of each of these lineages using variant-specific estimated infections
112 from the covidestim model. For this, we partitioned the covidestim weekly estimated COVID-19
113 infections in Connecticut based on state-wide variant frequency to calculate variant-specific
114 reproduction numbers (R_t) over the course of 2022 **(Fig 2C)**. We show that although BA.1 had the
115 highest initial R_t value (2.4, CrI 1.6-3.5), it quickly fell below 1 in early January. BA.2 emerged in
116 February 2022 with an initial R_t of 1.7 (CrI 1.3-2.2), followed by a notable decrease and a plateau at
117 around 1.2 for several weeks before falling below 1 around April 2022. The initial R_t of BA.5 (1.5 CrI
118 1.2-1.86) and BA.4 (1.2 CrI 1.07-1.36) were overall lower than for BA.1 and BA.2. However, BA.4
119 and BA.5 both hovered at $R_t \sim 1$ for several months during summer 2022. BA.4 was finally outcompeted
120 by late-stage BA.5 lineages. The R_t for BA.5 fell below 1 once XBB was introduced with an R_t of 1.4
121 (CrI 1.1-1.7). The R_t of XBB fell below 1 around the beginning of 2023.

122 Next, we sought to understand the relative transmission advantages during the emergence periods by
123 comparing R_t values of co-circulating lineages (**Fig 2D**). We first identified 14-day windows in which
124 one lineage replaced the previously dominating lineage (**Supplementary Table 1**). Using a method
125 previously developed (Earnest et al. 2022; Petrone et al. 2022), we identified six, 14-day periods of
126 variant overlap and divided the R_t value of the emerging lineage by the R_t value of the previously
127 dominating lineage for each day of the emergence period, yielding 14 R_t ratios. The median of these
128 values results in a comparative fitness measure (**Fig 2D**). We show that BA.1 and BA.2 were 78.4%
129 and 76% more transmissible than Delta and BA.1, respectively (**Fig 2D**). The advantage of both BA.4
130 and BA.5 over BA.2 was significantly lower at 27.9% and 48.5%, respectively. While BA.5 had a slight
131 fitness advantage of 10% over BA.4 during the emergence of both lineages, this advantage was not
132 sufficient to fully outcompete BA.4 for several months. However, late-stage BA.5 sub-lineages such as
133 BQ.1.1 and BF.7 (**Table 1**) were able to push out BA.4 before XBB emerged by late November. XBB
134 replaced these late-stage BA.5 sequences with a fitness advantage of 28.5%.

135 By characterizing the growth rates during the emergence windows for the major Omicron lineages, we
136 have shown high variance in lineage replacement dynamics. The lack of a trend in our R_t ratio analysis
137 suggests the fitness advantages of incoming lineages are likely being influenced by several non-uniform
138 factors that vary for different emergence windows. We next sought to further dissect these observations
139 through exploring possible underlying drivers of the incoming lineages' fitness advantages.



140

141 **Fig 2. Comparison of key epidemiological parameters for each Omicron lineage in 2022.** (A) Frequencies of the
 142 incoming Omicron lineage during its emergence period highlight the time interval between being detected at 5% and
 143 50% of all sequences (based on GISAID data for Connecticut). (B) Comparison of growth rates between the different
 144 Omicron lineages and the average slope of the growth curve during emergence periods (C) Variant-specific R_t numbers
 145 for each of the Omicron lineage over time derived from the modeled overall R_t from the covidestim model (D) Based
 146 on (C), the R_t ratios for each of the emergence periods were calculated to estimate the average advantage of each
 147 incoming lineage compared to the previously dominating one.

148

149 **Average inter- and intra-lineage viral copy numbers vary over time and**
150 **only partially explain lineage replacement patterns**

151 To explain the specific mechanisms by which variants gain advantages over another, we evaluated the
152 fitness advantage of each variant as a combination of intrinsic transmissibility and immune escape. For
153 the purpose of this study, we used proxies derived from data collected through our genomic surveillance
154 program for each of these factors.

155 As a proxy for intrinsic transmissibility, we measured virus copies in nasopharyngeal swab material
156 using RT-qPCR. We used the same assay (Vogels et al. 2021) for each sample processed for sequencing
157 which enables us to compare average cycle threshold (Ct) values per variant across a total of 11,111
158 samples (**Fig 3A**). We also converted the RT-qPCR values to genome equivalents (**Supplementary**
159 **figure 3**).

160 Using cross-sectional data has caveats and is sensitive to several epidemiological and viral factors
161 (Fryer et al. 2023; Hay et al. 2021). Changes in tissue tropism, symptom severity, and test-seeking
162 behavior are expected to differ for Omicron infections compared to infections with pre-Omicron
163 lineages. In the following, we are thus focusing on Omicron-lineage samples only.

164 For this, we analyzed 6,856 samples identified as Omicron-lineages (**Fig 3B**) collected from a wide
165 range of individuals and disease statuses, including asymptomatic individuals detected through baseline
166 surveillance of outpatients as well as inpatients and emergency department visits. We were particularly
167 interested in Ct-value trends over time and plotted the raw data with temporal resolution (**Fig 3C**). We
168 then tested the data for the assumptions of linearity and fit linear regressions (**Fig 3D**) to derive
169 coefficients as a measure of Ct-value change over time for each lineage (**Table 2**).

170 *Table 2 Trends in median Ct values of the major Omicron lineages over time*

Lineage	Median Ct early samples	Median Ct late samples	Regression Coefficient (Ct / day) (p-value)
BA.1	27.297 (IQR: 24.179 - 30.918)	27.799 (IQR: 26.139 - 28.760)	+0.016 (0.045)
BA.1.1	25.637 (IQR: 22.8- 28.15)	28.399 (IQR: 25.563, 30-184)	+0.016 (0.011)
BA.2	26.681, IQR: 22.557 - 29.128	22.544 (IQR: 20.304, 25.718)	-0.015 (0.002)
BA.2.12.1	22.972 (IQR: 22.928 - 22.540)	23.335 (IQR: 22.928 - 22.540)	-0.021 (<0.001)
BA.4	21.2 (IQR: 18.944 - 23.75)	19.379 (IQR: 19.088 - 21.132)	+0.022 (0.227)
BA.5	23.077 (IQR: 19.61 - 25.606)	25.131 (IQR: 22.750 - 28.133)	+0.015 (<0.001)
BQ.1.1	23.231 (IQR: 21.580 - 24.561)	25.828 (IQR: 23.446 - 29.863)	+0.005 (0.758)
XBB	21.794 (IQR: 20.573 - 26.42)	24.753 (IQR: 19.846 - 27.566)	+0.03 (0.024)

171 Looking at trends over time, we noticed that the average Ct value for BA.1, BA.4, BA.5, and XBB
 172 samples increased over time (decreasing viral copy numbers) towards the end of each wave with a rate
 173 around 0.015-0.03 Ct values/day (**Table 2**). However, for the BA.2 and BA.2.12.1 samples, we
 174 observed a decreasing trend towards the end of the BA.2 wave with a decrease of 0.015 and 0.021 Ct
 175 values/day.

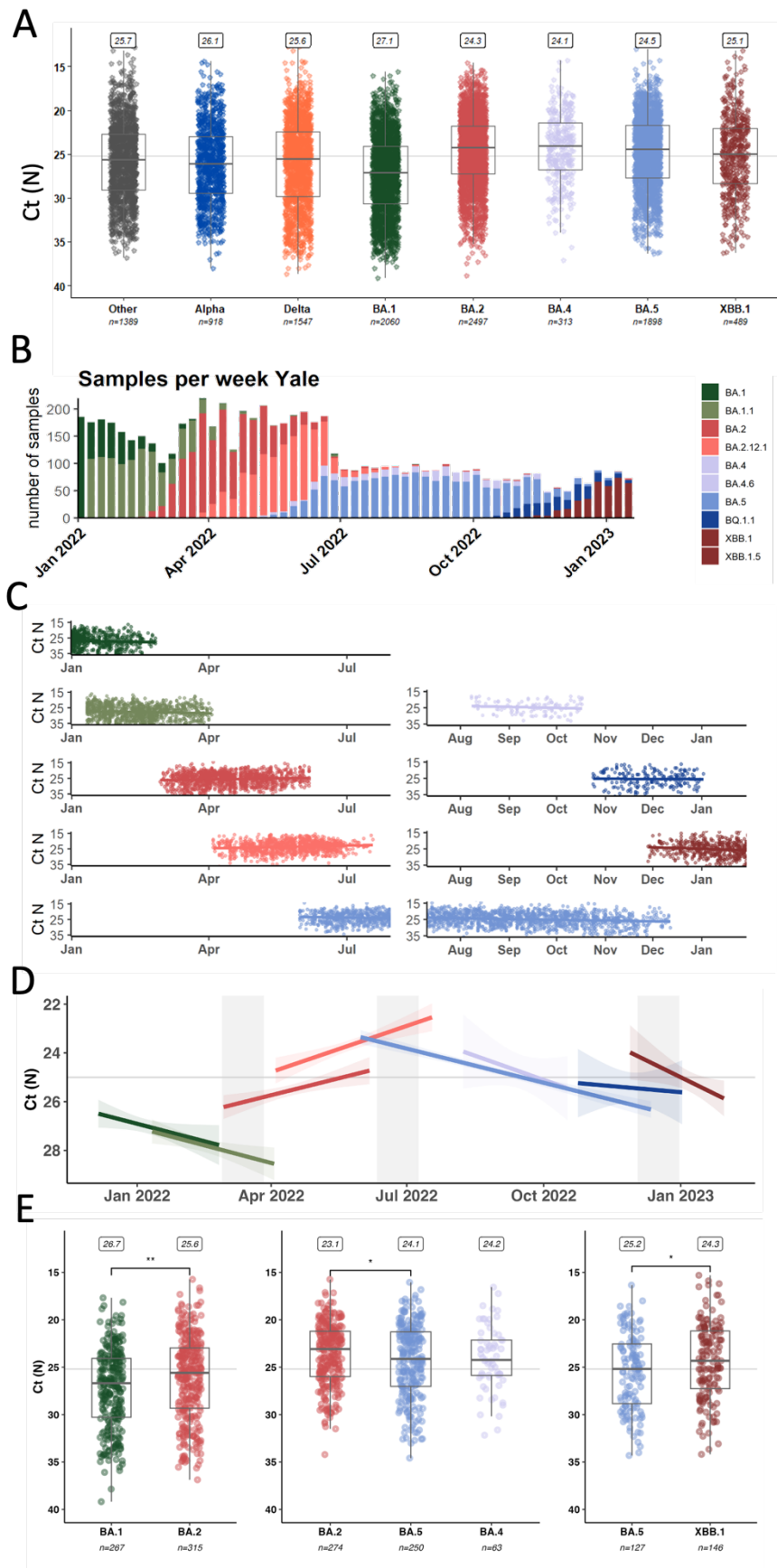
176 Next, we compared only samples that were collected specifically during the emergence period of an
 177 incoming lineage, defined as 14 days on either side of the date where the previously dominant and the
 178 incoming variant each account for 50% of the samples (**Supplement Table 2**).

179 Early BA.2 samples had significantly lower Ct values (median 25.6, Interquartile Range (IQR) 23.0-
 180 29.3) compared to late BA.1 samples (median 26.7, IQR 24.1-30.3) (p-value: 0.003) (**Fig 3E**). This
 181 supports previous reports from two European surveillance programs that also showed higher viral copies

182 of BA.2 over BA.1 as measured by qPCR (Lentini et al. 2022; Musalkova et al. 2023). When looking
183 at the emergence period of BA.4 and BA.5 compared to late-stage BA.2 samples, samples infected with
184 the incoming variant had significantly higher Ct values than BA.2 samples (BA.4 median 24.2, IQR
185 22.1-25.9; BA.5 median 24.1, IQR 21.3-27.0, BA.2 median 23.1, IQR 21.2-26.0) from that same period
186 (p-value: 0.034). There was no statistically significant difference in the Ct values between BA.4 and
187 BA.5 samples (p-value: 0.829). Finally, early XBB samples again had lower Ct values (median 24.3,
188 IQR 21.2-27.3) compared to late-stage BA.5 samples (including BQ.1.1) (median 25.2, IQR 22.5-28.8)
189 (p-value: 0.033).

190 We also sought to investigate whether there was any association of patient metadata with Ct value in
191 these first XBB cases by stratifying the samples according to age, sex, vaccination status, and patient
192 class (**Supplementary Figure 4**). There was no significant difference in Ct values based on vaccination
193 status. However, we found that people admitted to the emergency department had, on average, lower
194 Ct values compared to those tested as inpatients or outpatients.

195 In summary, using an RT-qPCR assay for assessing viral copy number for each sample we submitted
196 to whole-genome sequencing, we revealed striking temporal patterns. A higher viral copy number was
197 not necessarily decisive for a lineage's fitness advantage as, for example, incoming BA.5 samples had
198 lower viral copy numbers than late BA.2 samples. Together, this hints at a varying advantage conferred
199 by enhanced intrinsic transmissibility, as measured by viral copy numbers, that changed over the course
200 of the year and seems mostly linked to BA.2-derived lineages.



202 **Figure 3 Comparing average qPCR Ct values as a proxy for variant intrinsic transmissibility. (A)** Summary of all
203 samples processed in our genomic surveillance programme from 2021 to January 2023 **(B)** Overview about the numbers
204 and distribution of Omicron samples **(C)** Ct values from Omicron samples plotted together with modeled average over
205 time **(D)** Based on (C), summary values for each of the Omicron lineages with emergence periods highlighted **(E)**
206 Statistical analysis of Ct values retrieved from samples collected during the emergence periods.

207 **Likelihood of incoming lineages to cause breakthrough infections in recent** 208 **vaccinees varies across different Omicron lineages**

209 As BA.4 and BA.5 replaced BA.2 without clear advantage in their viral copy numbers, we next sought
210 to assess the immune escape capacity to circumvent vaccine-induced immunity as another potential
211 feature to increase a variant's fitness.

212 A blood donor seroprevalence survey showed that in December 2021, 95.5% of donors (95%
213 Confidence Interval (CI) 93.5-96.9%) had antibodies against the Spike antigen, compared to 17.8% (CI
214 15.3-20.5%) with infection-induced antibodies (Busch et al. 2022; Jones et al. 2022). The US CDC
215 reports high vaccination coverage in Connecticut (70% coverage with 2 doses in September 2021) as
216 well as uptake of a third dose booster towards the end of 2021 (55% in January 2022) (**Fig 4A**). Further,
217 bi-valent booster shots (Wuhan-Hu-1+BA.5) were administered to 23% of the population (**Fig 4A**).
218 During 2022, the estimated proportion of individuals with at least one previous SARS-CoV-2 infection
219 passed 75% in July (Klaassen et al. 2022, 2023) (**Fig 4B**). Thus, the pool of antigen-naïve hosts was
220 greatly depleted towards mid-2022. Consequently, the fitness advantage of variants being able to escape
221 from this high population immunity were expected to increase over time (**Fig 4B**). Accordingly, in
222 experimental assays with serum collected from curated cohorts with defined antigen exposures,
223 Omicron lineages BA.1, BA.2, BA.5 and XBB showed an astounding sequential drop in sensitivity to
224 neutralization by vaccine- and infection induced antibodies (Cao et al. 2023; Mykytyn et al. 2023a,b;
225 Rössler et al. 2022).

226 To examine how immune escape contributed to the fitness advantages of incoming Omicron lineages,
227 we compared the likelihood of the incoming lineage to cause more vaccine breakthrough infections
228 (BTI) than the dominant lineage during a five-week window of variant emergence (**Supplement Table**
229 **3**). We fitted mixed-effect multivariable logistic regression models adjusted for several potential
230 confounding variables, including vaccination status, sex, age, location, and calendar time.

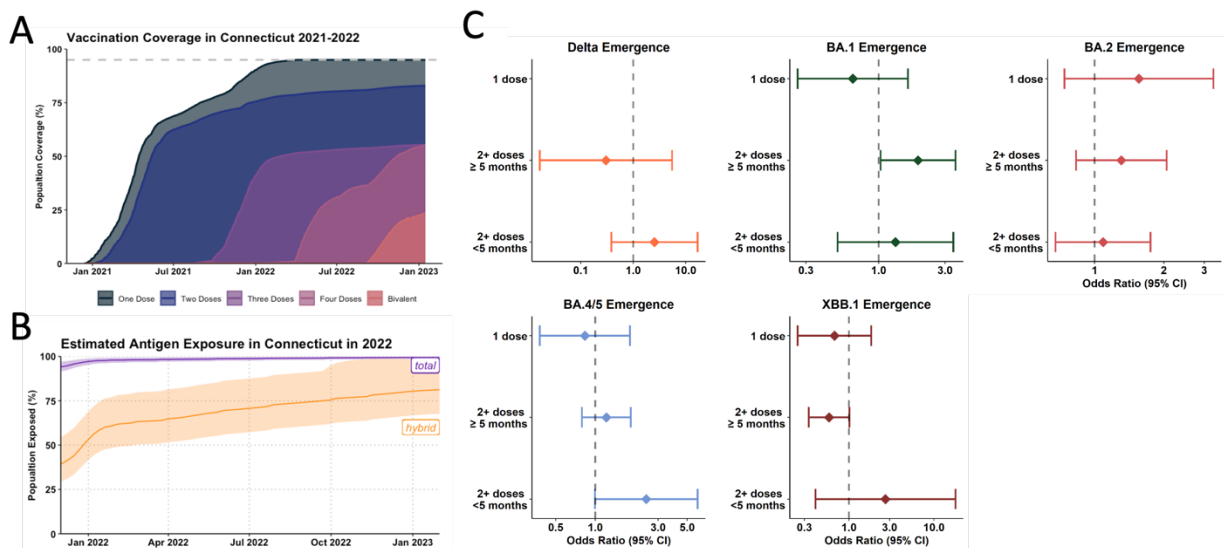
231 We show an increased odds of being infected with BA.1 compared to Delta amongst those vaccinated
232 with at least 2 doses and who were more than 5 months from their most recent vaccination (OR: 1.92,
233 95% CI: 1.03 - 3.56) (**Fig 4C**). Thus, enhanced immune escape played a role in the emergence of BA.1
234 while not being a significant driver of fitness advantage in the emergence of Delta in 2021. This result
235 is in line with our previous study based on a similar population that found enhanced odds of being
236 infected with Omicron BA.1 in triple-vaccinated individuals (Chaguza et al. 2022).

237 For the emergence of BA.2, we did not find overrepresentation in causing breakthrough infections
238 during its emergence period, likely suggesting little to no effect of immune escape in our model (**Figure**
239 **4C**). During the emergence of BA.5, we found a tendency for an increased risk of having been infected
240 with BA.5 vs. BA.2 when having been vaccinated in the last 5 months prior to infection (OR: 2.441,
241 95% CI: 0.995 - 5.988), though this did not reach statistical significance (**Figure 4C**). Finally, for the
242 emergence of XBB, we found a tendency for a decreased likelihood of being infected with XBB
243 amongst those who are more than 5 months from their most recent vaccination (OR: 0.586, 95% CI:
244 0.339-1.013) albeit this did not reach statistical significance in our analysis (**Figure 4C**).

245 While these models are limited in understanding vaccine breakthrough infections from a population-
246 level rather than mechanistic perspective, various in-vitro studies lend support to and provide context
247 for our findings. Notably, the seeming lack of vaccine effects in the emergence of BA.2 can be explained
248 by the low antigenic distance between BA.2 and BA.1, especially in people having received 3
249 monovalent doses (Arora et al. 2022b; Hoffmann et al. 2022; Kurhade et al. 2022; Tan et al. 2022).
250 Additionally, several vaccine cohort studies have shown that BA.5 is more immune-evasive than BA.2
251 (Arora et al. 2022a; Cao et al. 2022b; Hoffmann et al. 2023b). The lack of statistical significance seen

252 for the emergence of BA.5 in our analysis may be attributable to the comparatively small sample size
 253 for these strata in our dataset (**Supplement Table 10**).

254 Our analysis shows that the advantage an emerging lineage gained through immune escape varies over
 255 time and that in-vitro findings may not fully translate to a heterologous immunity landscape influenced
 256 by individual combinations of infections, boosters, shifts in test-seeking behavior, and other population-
 257 level factors.



258
 259 **Figure 4 Influence of vaccine uptake and community-immunity levels on Omicron lineage emergence. (A)**
 260 Vaccination coverage of Connecticut as reported by the US CDC for 2021 and 2022 **(B)** Estimated antigen exposure
 261 based on estimates from covidestim model according to either total (vaccination and/or infection) (purple) and hybrid
 262 exposure (infection and/or vaccination) (orange) **(C)** Logistic regression model to compare the ratios of infections
 263 caused by the incoming or previously dominant variant based on vaccination status during the emergence windows.
 264 BA.4 and BA.5 were analyzed together due to the similarity in the Spike region.

265 **A conceptual model describing Omicron lineage fitness in a highly dynamic** 266 **fitness landscape**

267 Lastly, we explored how the infection dynamics of each variant influenced the emergence of the
268 subsequent replacement variant. For this, we analyzed population-level immune exposure by
269 calculating the number of infections 60-, 90-, or 120-days prior to the time point where an incoming
270 lineage reached 5% of sequence frequency (**Fig 5A**). Emerging BA.2 lineages in March 2022 faced a
271 population that experienced around 1.5 million BA.1 infections within the last 90 days, the time frame
272 where antibody-mediated protection against re-infections is expected to be highest. For the emergence
273 of BA.5 and XBB, this figure was around 0.7 million. This extensive infection dynamic led to a gradual
274 rise in the proportion of Connecticut's population that was protected against reinfection as estimated
275 through the covidestim model (**Fig 5B**) (Klaassen et al. 2022, 2023). Based on these estimates, we
276 schematically plotted the relative importance of either intrinsic transmissibility or antigenic distance for
277 an emerging variant's fitness advantage over the course of 2022 (**Fig 5C**). While immune escape
278 increases gradually, following the number of people with Omicron antigen exposure, the advantage
279 conferred through higher intrinsic transmissibility mainly played a role after the BA.1 and BA.5 waves,
280 which infected up to 50% of the population each.

281 Summarizing our findings presented here, together with evidence from the literature, we developed a
282 conceptual model based on a classical susceptible, infected, and recovered (SIR) compartmental
283 dynamic transmission model highlighting fitness determinants of Omicron lineages (**Fig 5D**). Since
284 Omicron BA.1 encompassed a vastly divergent Spike protein from pre-Omicron viruses, the previously
285 observed high efficacy of vaccines, especially mRNA-platform based formulations, was greatly
286 diminished (Andrews et al. 2022; Cao et al. 2022; Cele et al. 2022; Garcia-Beltran et al. 2022). In the
287 model, this is reflected by opening a novel antigenic space (also defined as serotype) compared to
288 previous pre-Omicron lineages (Simon-Loriere & Schwartz 2022). We include three different levels of
289 susceptibility depending on vaccine status (S_N , S_V , S_{V3+}), as these strata have shown to harbor different
290 quantities and qualities in antibody levels and thus protection against a first Omicron infection

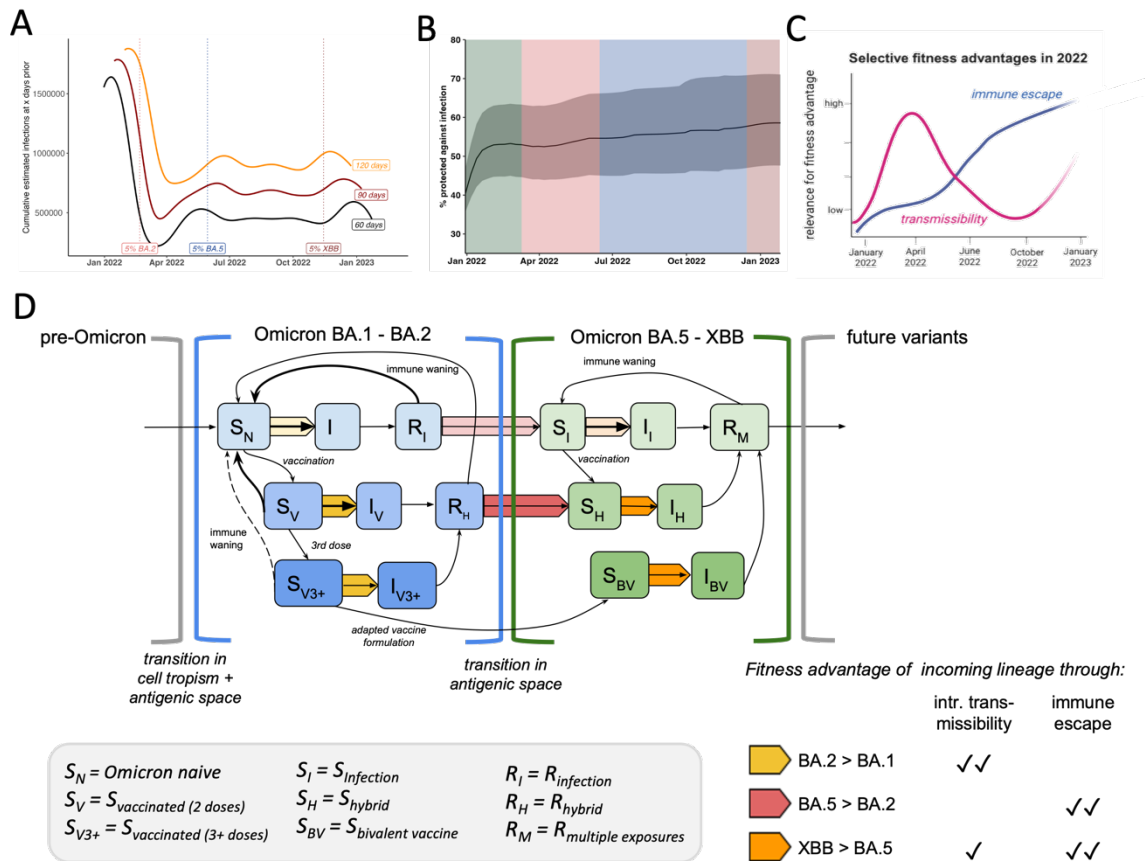
291 (Muecksch et al. 2022; Park et al. 2022; Schaefer-Babajew et al. 2022). The exploration of this new
292 antigenic space confers a fitness advantage in itself, moving 40-50% of Connecticut's population from
293 the 'susceptible' (S_N = Omicron-naive, i.e. no previous Omicron antigen exposure) compartment to
294 'recovered' (R_I for unvaccinated or R_H for vaccinated).

295 The fraction of the population that just recovered from BA.1 (**Fig 5A**) was likely fairly well protected
296 against a swift reinfection with either BA.1 or the antigenically similar BA.2 (Zhou et al. 2023). Based
297 on epidemiological data, the transition from the R_I/R_H bin back to the 'susceptible' bin within the same
298 antigenic space takes around 6 months (Andeweg et al. 2023; Malato et al. 2023; 2023). BA.2 was
299 competing with BA.1 to infect the remaining 'susceptible' population (i.e. Omicron-naive S_N) fraction
300 of the population. Based on our analysis, we conclude BA.2 outcompeted BA.1 in reaching this
301 susceptible population faster through its higher intrinsic transmissibility (yellow arrow) (**Figs 3E and**
302 **5D**).

303 After the BA.1 and BA.2 waves, approximately one-third of the population remained in the Omicron-
304 naive compartment (**Fig 1D**). The fitness advantage of variants in the same antigenic space, even with
305 higher transmissibility (like BA.2.12.1), was restricted to this remaining pool of susceptibles. BA.4 and
306 BA.5 successfully escaped from immunity conferred through pre-Omicron antigen contacts as well as
307 BA.1/BA.2 infections and thus opened a second antigenic space (**Fig 5D**). Vaccinated or previously
308 infected individuals fall back from being fairly protected ('recovered' bin) in the previous antigenic
309 space to the 'susceptible' (S_I, S_H) state in the second antigenic space (**Fig 5D**). Although BA.4 and BA.5
310 displayed lower intrinsic transmissibility compared to BA.2 (**Fig 3D**), these variants outcompeted BA.2
311 as they could spread in a larger fraction of people (the R_I & R_H bins) (red arrow) (**Fig 5D**). The fairly
312 high and steady transmission levels of BA.4 and 5 (**Fig 1C**) were likely defined by the rate of individuals
313 moving from the recovered bin of the first antigen space to the S compartment in the second antigenic
314 space (**Fig 5D**).

315 At the time XBB emerged, over 80% of the population had at least one Omicron antigen exposure (**Fig**
316 **4B**). For the purpose of our model, we assume that XBB covers a similar antigenic niche as BA.5.
317 Although XBB displays immune evasion from BA.5-induced immunity, some cross-neutralization,
318 especially in individuals with previous Omicron antigen contact, was reported (Kurahade et al. 2023;
319 Springer et al. 2023). In order to outcompete the ongoing BA.5 transmission chains (**Fig 2D**), any
320 incoming lineage had to maintain at least similar or higher levels of immune escape while also being
321 more transmissible (orange arrow) (**Fig 5D**). Thus, XBB outcompeted late-stage BA.5 samples through
322 its extensive immune escape profile (Hoffmann et al. 2023) paired with higher intrinsic transmissibility
323 (**Fig 3E**) and thus spreading faster within the susceptibles in the second antigenic space (**Fig 5D**).

324 In summary, we provide a framework to assess critical parameters that define variant fitness of Omicron
325 lineages in 2022. Ongoing SARS-CoV-2 evolution led to the emergence of lineages with greater
326 flexibility in exploring different fitness niches in a highly dynamic host population through a differential
327 combination of intrinsic transmissibility and immune escape.



328

329 **Figure 5 Summary of selective fitness advantages of Omicron lineage emergence in a dynamic host immunity**

330 **landscape. (A)** Sliding-window analysis of cumulative estimated infections 60, 90 or 120 days prior to each date on the

331 plot with highlights when emerging Omicron lineages reached 5% of total samples **(B)** Frequency of estimated % of the

332 population thought to be protected against infection based on vaccine and or infection status based on the covidestim

333 model **(C)** Conceptual visualization of selective advantages of incoming Omicron lineages over the year **(D)** SIR-based

334 conceptual transmission model highlighting different fitness advantages of incoming Omicron lineages depending on

335 the status of the host population. Shades of yellow, orange and red represent the different combinations of advantageous

336 fitness traits as outlined in the table in the right corner.

337

338 **Discussion**

339 We evaluated the underlying drivers of fitness advantages that led to the sequential sweeps of Omicron
340 lineages in Connecticut during 2022. By determining selective traits that best explain the observed
341 lineage dynamics, our analysis revealed the ability of SARS-CoV-2 lineages to thrive in a variety of
342 highly dynamic fitness landscapes. A key result from the data presented here is that SARS-CoV-2
343 fitness was not dictated by a single factor, but rather a fine-tuned combination of intrinsic
344 transmissibility and immune escape. This intrinsic volatility of the fitness landscape is, by definition,
345 coupled with the antigen exposure history of the host population, making fitness advantages moving
346 targets.

347 While novel virus lineages are designated according to their phylogenetic identity, inferring
348 epidemiological relevance and antigenic space from genetic data alone remains challenging. Thus, in
349 addition to continuing efforts of genomic surveillance, it remains crucial to collect relevant clinical and
350 epidemiological patient data, ideally coupled with broad-scale and representative sero-prevalence
351 surveys. Being able to link genetic information with additional laboratory and epidemiological data of
352 locally matched host-pathogen populations and their epidemic outcomes is crucial for evaluating the
353 potential of novel variants (Meijers et al. 2023).

354 2022 was unique in terms of the spread of the Omicron family, followed by highly synchronized antigen
355 exposures resulting in fairly homogenous population-level immunity. Going forward, the immunity
356 landscape will likely greatly diversify depending on individuals' antigen exposure histories and on the
357 synchronicity of waning rates between individuals. This has implications for future SARS-CoV-2
358 transmission as a significant portion of the population might become susceptible to newly circulating
359 lineages entering the northern hemisphere winter season of 2023/2024. We showed that in 2022, high
360 levels of population immunity towards the end of the year slowed down the growth rates of BA.5 and
361 XBB. Thus, variant-turnovers will take longer in future and might be more subtle than the rapid lineage

362 displacements in 2022. Additionally, the high number of co-circulating XBB-variants might further
363 limit the growth rates of newly emerging variants (Beesley et al. 2023).

364 We demonstrate the utility of an integrated approach to genomic surveillance data collection for
365 identifying key characteristics of SARS-CoV-2 fitness dynamics. Data linkage to key patient metadata
366 was crucial to evaluate existing data from laboratory studies and curated vaccinee cohorts in a real-
367 world, population-level setting and should be considered when designing surveillance systems. Such
368 frameworks provide critical infrastructure to evaluate emerging lineages of known and unknown
369 pathogens and can be further incorporated into tailoring public health responses and informing vaccine
370 formulations. Lessons learned from SARS-CoV-2 can be utilized and further adapted to other pathogens
371 to maximize the usefulness of such surveillance programmes for community health.

372 This retrospective analysis re-visits the lineage replacement dynamics of Omicron lineages that
373 dominated Connecticut in 2022 and sheds light on the underlying drivers of their sequential fitness
374 advantages. This study exemplifies a use-case for combining sequencing data with epidemiological and
375 laboratory metadata to better understand pathogen emergence. Based on the high-level data used in this
376 study, we showcase that linking vaccination status and viral copy numbers to genomic surveillance data
377 may provide crucial tools to evaluate variant fitness for SARS-CoV-2 and beyond.

378 **Limitations**

379 One limitation of this study might be the validity of these findings to other populations and settings. As
380 outlined above, variant transmission advantages are intrinsically coupled to the local host population
381 and thus our results are most applicable to other places with similar population characteristics,
382 vaccination uptake rates, and public health policies. Whereas the specific dynamics of the different
383 Omicron waves may vary locally, the data presented here is valuable for examining overall trends that
384 are broadly applicable to other settings. Overall fitness advantages of each new Omicron lineage over
385 their respective predecessor were fairly consistent globally as recently shown when analyzing different
386 settings globally (Meijers et al. 2023).

387 A further potential limitation is that our dataset for Ct value comparison is based on a pre-selection from
388 the overall pool of available SARS-CoV-2 positive samples based on a Ct value cut-off in the diagnostic
389 test that were expected to yield high sequencing coverage. We think this reflects the proportion of
390 samples that would possess the viral burden that is relevant for onward transmission and thus suitable
391 for the purpose of this study. Further, it could be argued that Ct values do not necessarily scale with the
392 amounts of infectious viral particles and that the kinetics of RNA clearance may not be directly related to
393 clearance of infectious virus. For our specific assay, we used a standard curve to convert Ct values to
394 absolute viral genome copies and we are usually able to isolate infectious virus from samples with Ct
395 values below 30 (based on internal data). Further, symptom severity is thought to have remained similar
396 over all Omicron lineages, reducing the potential for bias due to differences in test seeking behavior.
397 Lastly, for the purposes of this study, we were interested in comparing trends between lineages in
398 contrast to absolute values.

399 **Materials & Methods**

400 **Ethics statement**

401 The Institutional Review Board from the Yale University Human Research Protection Program
402 determined that the RT-qPCR testing and sequencing of de-identified remnant COVID-19 clinical
403 samples obtained from clinical partners conducted in this study is not research involving human subjects
404 (IRB Protocol ID: 2000028599).

405 **Data sources**

406 **Clinical sample collection, RT-qPCR, and sequencing**

407 SARS-CoV-2 positive samples (nasal swabs in viral transport media) were collected through the Yale
408 New Haven Hospital (YNHH) System as a part of routine inpatient and outpatient testing and sent to
409 the Yale SARS-CoV-2 Genomic Surveillance Initiative. Using the MagMAX viral/pathogen nucleic
410 acid isolation kit, nucleic acid was extracted from 300 μ l of each clinical sample and eluted into 75 μ l of
411 elution buffer. Extracted nucleic acid was then tested using a “research use only” (RUO) RT-qPCR
412 assay (Vogels et al. 2021) for SARS-CoV-2 RNA. Libraries were prepared for sequencing using the
413 Illumina COVIDSeq Test (RUO version) and quantified using the Qubit High Sensitivity dsDNA kit.
414 Negative controls were included for RNA extraction, cDNA synthesis, and amplicon generation.

415 Prepared libraries were sequenced at the Yale Center for Genomic Analysis on the Illumina NovaSeq
416 with a 2x150 approach and at least 1 million reads per sample.

417 Reads were then aligned to the Wuhan-Hu-1 reference genome (GenBank MN908937.3) using BWA-
418 MEM v.0.7.15 (Li 2013). Adaptor sequences were then trimmed, primer sequences masked, and
419 consensus genomes called (simple majority >60% frequency) using iVar v1.3.133 (Grubaugh et al.
420 2019) and SAMtools (Danecek et al. 2021). When <20 reads were present at a site an ambiguous “N”
421 was used, with negative controls consisting of \geq 99% Ns. The Pangolin lineage assignment tool
422 (O’Toole et al. 2021) was used for assigning viral lineages.

423 **Clinical metadata**

424 We obtained patient metadata and vaccination records from the YNHH system and the Center for
425 Outcomes Research and Evaluation (CORE) and matched these records to sequencing data through
426 unique sample identifiers. Duplicate patient records or those with missing or inconsistent vaccination
427 data were removed. We determined vaccination status at time of infection by comparing the sample
428 collection date to the patient's vaccination record dates.

429 We then categorized vaccine breakthrough statuses with respect to both the number of vaccine doses
430 received more than 14 days prior to the collection date and the timing of the most recent vaccination
431 relative to a 5 month period of time. Patient vaccination statuses at time of infection were thus
432 categorized as: non-vaccine breakthrough, one dose vaccine breakthrough, two or more dose vaccine
433 breakthrough greater than 5 months since the most recent vaccination, or two or more dose vaccine
434 breakthrough within 5 months since the most recent vaccination.

435 **Population vaccination trends**

436 We obtained data on vaccination trends in Connecticut from the Centers for Disease Control and
437 Prevention (CDC) (CDC 2021).

438 **Population variant trends**

439 We obtained variant trend data for Connecticut from the Global Initiative on Sharing All Influenza Data
440 (GISAID).

441 **Variant R_t and immunity estimates**

442 We obtained variant cumulative estimated case counts from covidestim, a Bayesian nowcasting
443 approach that incorporates reported cases, hospitalizations, immunity (Klaassen et al. 2022, 2023),
444 exposures, and vaccination data to generate state and county level estimates of variant specific
445 infections (Chitwood et al. 2022). To obtain variant-specific R_t estimates, we used the variant-specific
446 infection estimates from covidestim with the EpiEstim R package (Nouvellet et al. 2018).

447 **Analyses**

448 **Variant R_t ratios**

449 To compare R_t values between variants, we first selected 14-day periods when a new variant was
450 emerging in the population. For each of these time periods, we then divided the daily R_t value of the
451 emerging variant by the R_t value of the established variant for the same calendar day to calculate daily
452 R_t ratios.

453 **Variant emergence periods and logistic growth rates**

454 To determine the length of time each variant needed to become established in the population, we
455 calculated daily frequencies for each variant across Connecticut using case count data from GISAID.
456 We then defined a variant's emergence period as the date from when a variant first accounted for 5%
457 of all cases to the first date the variant reached its maximum frequency in the population. We then fitted
458 a locally estimated scatterplot smoothing (loess) curve to the data and extracted the fitted value
459 corresponding to a frequency of 50% in the population. With this value we determined the number of
460 days it took each variant to increase from a frequency of 5% in the population to 50%.

461 Using the same emergence periods, we fitted binomial logistic regression models where the variant
462 lineage was modeled as a function of calendar time. For each model, the variant(s) being displaced in
463 the population served as the reference group. We then extracted the coefficient of the predictor variable
464 of each model to determine the logistic growth rate for each variant.

465 **Variant C_t values over time and in periods of emergence**

466 To understand how C_t values change across time, we subset each variant to the period of time where it
467 was above 10% frequency in the population using RT-qPCR data from the Yale SARS-CoV-2 Genomic
468 Surveillance Initiative. For each of these time periods and variants we tested for heteroscedasticity via
469 a Breusch-Pagan test, checked for non-linearity or outlier values by plotting the residual values against

470 the fitted values, and tested for normality via a Q-Q plot and frequency histogram of model residuals.
471 We then fitted linear regression models where the Ct value was modeled as a function of calendar time.
472 To compare Ct values between variants, we identified 3, 4-week periods of variant co-circulation using
473 the same dataset. For the two periods of pairwise comparisons, we performed Wilcoxon rank sum tests.
474 For the comparison between three variants, we performed a Welch's ANOVA test as well as a one-way
475 ANOVA test to test for concordance, followed by post-hoc pairwise tests via Tukey's honest
476 significance test.

477 **Mixed effect multivariable logistic regression models**

478 To determine the impact of vaccinations in periods of variant emergence, we used sequencing data from
479 the Yale SARS-CoV-2 Genomic Surveillance Initiative matched to vaccination data from the YNH
480 System and CORE to identify five, five-week periods of variant co-circulation. We selected the specific
481 date ranges of these periods so as to balance the number of unvaccinated individuals attributed to each
482 variant in each period.

483 For these five periods we then fit mixed effect multivariable logistic regression models with a
484 dichotomous outcome of the co-circulating variants found in each time period. To dichotomize the
485 outcome in periods when more than two variants were circulating, we aggregated variants that emerged
486 or were displaced contemporaneously, with the reference set as the variant(s) that was being displaced
487 in the population.

488 Model covariates were selected via an Akaike information criterion (AIC) selection criteria test and
489 included vaccination status at the time of infection, patient sex (male or female), age (5-17, 18-39, 40-
490 64, 65+), town of residence as a random effect, and calendar time as a linear predictor. Non-vaccine
491 breakthrough, male sex, and the 18-39 age group served as variable reference levels. Due to the inability
492 for under 5 years olds to receive vaccinations for the majority of our study period, we restricted our
493 analysis to individuals 5 years and older.

494 To test the impact of the date interval lengths, we performed a sensitivity analysis by modifying the
495 period of emergence from 5 weeks to 3,4,6,7, and 8 weeks and found minimal differences in the results.

496 **Factors impacting XBB.1.5 Ct values**

497 To investigate the factors that impact Ct values associated with the XBB.1 variant infections, we subset
498 sequencing data from the Yale SARS-CoV-2 Genomic Surveillance Initiative to only those infections
499 caused by lineages within the XBB.1 parent lineage. We then identified calendar time, sex (female or
500 male), patient class (inpatient, outpatient, or emergency), age (<18, 18-49, 50-69, 70+), and vaccination
501 status at time of infection as variables that could impact Ct values.

502 To understand the impact of calendar time, we tested for heteroscedasticity via a Breusch-Pagan test,
503 checked for non-linearity or outlier values by plotting the residual values against the fitted values, and
504 tested for normality via a Q-Q plot and frequency histogram of model residuals. We then fit a linear
505 regression model to the data with Ct value as a function of calendar time.

506 For the remaining variables we assessed the normality of the Ct value distributions via Shapiro-Wilk
507 tests and the variance of the Ct value distributions via Bartlett or F-tests. To test for differences in Ct
508 values by sex, we performed equal variance t-tests. For the remaining variables, we performed Welch's
509 ANOVA tests as well as one-way ANOVA tests to test for concordance, followed by post-hoc pairwise
510 comparisons via Tukey's honest significance test.

511 **Conceptual SIR Model**

512 To synthesize our findings, we constructed a conceptual framework of variant fitness based on the
513 traditional SIR transmission model. As a conceptual framework, this model does not attempt to
514 explicitly simulate transmission through quantitative approaches. Rather, the model provides a visual
515 representation of the proposed mechanisms by which the Omicron lineages may have gained selective
516 advantages based on the results of our other analyses and findings from the literature.

517 **Statistical analysis and data availability**

518 We used the R statistical software (v. 4.2.1) (R Core Team (2021) R: A Language and Environment for
519 Statistical Computing. R Foundation for Statistical Computing, Vienna.) for all statistical analysis and
520 figures.

521 Data and code used in this study are publicly available on GitHub
522 (https://github.com/NickChen10/Omicron_project).

523 **Acknowledgments**

524 We gratefully acknowledge the work of all members of the Yale Genomic Surveillance Initiative
525 especially Center for Outcome Research at Yale New Haven Hospital. We thank all authors from the
526 originating laboratories responsible for obtaining the specimens, as well as the submitting laboratories
527 where the genomic data were generated and shared via GISAID. This project is supported by the CDC
528 Broad Agency Announcement Contracts 75D30122C14697 (awarded to NDG) and 75D30121C10273
529 (supports KF), the Connecticut Department of Public Health (CDPH) contract 21PSX0049 (awarded to
530 the Yale Center for Genome Analysis and supports NDG), and the Council of State and Territorial
531 Epidemiologists contract NU38OT000297 (supports KF). This work does not necessarily represent the
532 views of the CDC or CDPH.

533 **Author contribution:**

534 Conceptualization: NC, NDG, AMH

535 Methodology: NC, KP, NDG, AMH

536 Investigation: NC, KP, AMH, DMW, JLW, VP, NDG, RL, FK

537 Visualization: NC, KP, AMH

538 Funding acquisition: NDG

539 Supervision: NDG, AMH

540 Writing – original draft: NC, AMH

541 Writing – review & editing: all authors

542 **Competing Interests**

543 NDG is a paid consultant for BioNTech, DMW has received consulting fees from Pfizer, Merck, and
544 GSK, unrelated to this manuscript, and has been PI on research grants from Pfizer and Merck to Yale,
545 unrelated to this manuscript. JLW has received consulting fees from Pfizer and Revelar
546 Biotherapeutics Inc unrelated to this manuscript.

547 **References**

- 548 Andeweg SP, Gier B de, Vennema H, Walle I van, Maarseveen N van, et al. 2023. Higher risk of SARS-
549 CoV-2 Omicron BA.4/5 infection than of BA.2 infection after previous BA.1 infection, the Netherlands, 2
550 May to 24 July 2022. *Eurosurveillance*. 28(7):2200724
- 551 Andrews N, Stowe J, Kirsebom F, Toffa S, Rickeard T, et al. 2022. Covid-19 Vaccine Effectiveness against
552 the Omicron (B.1.1.529) Variant. *N. Engl. J. Med.* 386(16):1532–46
- 553 Arora P, Zhang L, Krüger N, Rocha C, Sidarovich A, et al. 2022a. SARS-CoV-2 Omicron sublineages show
554 comparable cell entry but differential neutralization by therapeutic antibodies. *Cell Host Microbe*.
555 30(8):1103-1111.e6
- 556 Arora P, Zhang L, Rocha C, Sidarovich A, Kempf A, et al. 2022b. Comparable neutralisation evasion of
557 SARS-CoV-2 omicron subvariants BA.1, BA.2, and BA.3. *Lancet Infect. Dis.* 22(6):766–67
- 558 Beesley LJ, Moran KR, Wagh K, Castro LA, Theiler J, et al. 2023. SARS-CoV-2 variant transition dynamics
559 are associated with vaccination rates, number of co-circulating variants, and convalescent immunity.
560 *eBioMedicine*. 91:104534
- 561 Brito AF, Semenova E, Dudas G, Hassler GW, Kalinich CC, et al. 2022. Global disparities in SARS-CoV-
562 2 genomic surveillance. *Nat. Commun.* 13(1):7003
- 563 Busch MP, Stramer SL, Stone M, Yu EA, Grebe E, et al. 2022. Population-weighted seroprevalence from
564 SARS-CoV-2 infection, vaccination, and hybrid immunity among U.S. blood donations from January-
565 December 2021. *Clin. Infect. Dis.: Off. Publ. Infect. Dis. Soc. Am.* 75(Supplement_2):ciac470
- 566 Cao Y, Jian F, Wang J, Yu Y, Song W, et al. 2023. Imprinted SARS-CoV-2 humoral immunity induces
567 convergent Omicron RBD evolution. *Nature*. 614(7948):521–29
- 568 Cao Y, Wang J, Jian F, Xiao T, Song W, et al. 2022a. Omicron escapes the majority of existing SARS-CoV-
569 2 neutralizing antibodies. *Nature*. 602(7898):657–63
- 570 Cao Y, Yisimayi A, Jian F, Song W, Xiao T, et al. 2022b. BA.2.12.1, BA.4 and BA.5 escape antibodies
571 elicited by Omicron infection. *Nature*. 608(7923):593–602
- 572 CDC. 2021. COVID-19 Vaccination Trends in the United States, National and Jurisdictional | Data | Centers
573 for Disease Control and Prevention
- 574 Cele S, Jackson L, Khoury DS, Khan K, Moyo-Gwete T, et al. 2022. Omicron extensively but incompletely
575 escapes Pfizer BNT162b2 neutralization. *Nature*. 602(7898):654–56
- 576 Chaguza C, Coppi A, Earnest R, Ferguson D, Kerantzas N, et al. 2022. Rapid emergence of SARS-CoV-2
577 Omicron variant is associated with an infection advantage over Delta in vaccinated persons. *Med (N. York,
578 Ny)*. 3(5):325-334.e4
- 579 Chitwood MH, Russi M, Gunasekera K, Havumaki J, Klaassen F, et al. 2022. Reconstructing the course of
580 the COVID-19 epidemic over 2020 for US states and counties: Results of a Bayesian evidence synthesis
581 model. *PLoS Comput. Biol.* 18(8):e1010465
- 582 Danecek P, Bonfield JK, Liddle J, Marshall J, Ohan V, et al. 2021. Twelve years of SAMtools and BCFtools.
583 *GigaScience*. 10(2):giab008
- 584 Earnest R, Uddin R, Matluk N, Renzette N, Turbett SE, et al. 2022. Comparative transmissibility of SARS-
585 CoV-2 variants Delta and Alpha in New England, USA. *Cell Reports Medicine*. 3(4):100583

- 586 Faria NR, Mellan TA, Whittaker C, Claro IM, Candido D da S, et al. 2021. Genomics and epidemiology of
587 the P.1 SARS-CoV-2 lineage in Manaus, Brazil. *Science*. 372(6544):815–21
- 588 Fryer HR, Golubchik T, Hall M, Fraser C, Hinch R, et al. 2023. Viral burden is associated with age,
589 vaccination, and viral variant in a population-representative study of SARS-CoV-2 that accounts for time-
590 since-infection-related sampling bias. *PLOS Pathog*. 19(8):e1011461
- 591 Garcia-Beltran WF, Denis KJSt, Hoelzemer A, Lam EC, Nitido AD, et al. 2022. mRNA-based COVID-19
592 vaccine boosters induce neutralizing immunity against SARS-CoV-2 Omicron variant. *Cell*. 185(3):457-
593 466.e4
- 594 GISAID. <https://gisaid.org>
- 595 Goh AXC, Chae S-R, Chiew CJ, Tang N, Pang D, et al. 2023. Characteristics of the omicron XBB subvariant
596 wave in Singapore. *Lancet*. 401(10384):1261–62
- 597 Grubaugh ND, Gangavarapu K, Quick J, Matteson NL, Jesus JGD, et al. 2019. An amplicon-based
598 sequencing framework for accurately measuring intrahost virus diversity using PrimalSeq and iVar. *Genome*
599 *Biol*. 20(1):8
- 600 Hay JA, Kennedy-Shaffer L, Kanjilal S, Lennon NJ, Gabriel SB, et al. 2021. Estimating epidemiologic
601 dynamics from cross-sectional viral load distributions. *Science*. 373(6552):eabh0635
- 602 Hill V, Plessis LD, Peacock TP, Aggarwal D, Colquhoun R, et al. 2022. The origins and molecular evolution
603 of SARS-CoV-2 lineage B.1.1.7 in the UK. *Virus Evol*. 8(2):veac080
- 604 Hoffmann M, Arora P, Nehlmeier I, Kempf A, Cossmann A, et al. 2023. Profound neutralization evasion
605 and augmented host cell entry are hallmarks of the fast-spreading SARS-CoV-2 lineage XBB.1.5. *Cell. Mol.*
606 *Immunol*. 20(4):419–22
- 607 Hoffmann M, Behrens GMN, Arora P, Kempf A, Nehlmeier I, et al. 2022. Effect of hybrid immunity and
608 bivalent booster vaccination on omicron sublineage neutralisation. *Lancet Infect. Dis*. 23(1):25–28
- 609 Jones JM, Opsomer JD, Stone M, Benoit T, Ferg RA, et al. 2022. Updated US Infection- and Vaccine-
610 Induced SARS-CoV-2 Seroprevalence Estimates Based on Blood Donations, July 2020–December 2021.
611 *JAMA*. 328(3):298–301
- 612 Klaassen F, Chitwood MH, Cohen T, Pitzer VE, Russi M, et al. 2022. Population Immunity to Pre-Omicron
613 and Omicron Severe Acute Respiratory Syndrome Coronavirus 2 Variants in US States and Counties
614 Through 1 December 2021. *Clin. Infect. Dis.: Off. Publ. Infect. Dis. Soc. Am*. 76(3):e350–59
- 615 Klaassen F, Chitwood MH, Cohen T, Pitzer VE, Russi M, et al. 2023. Changes in Population Immunity
616 Against Infection and Severe Disease From Severe Acute Respiratory Syndrome Coronavirus 2 Omicron
617 Variants in the United States Between December 2021 and November 2022. *Clin. Infect. Dis.: Off. Publ.*
618 *Infect. Dis. Soc. Am*. 77(3):355–61
- 619 Kurhade C, Zou J, Xia H, Cai H, Yang Q, et al. 2022. Neutralization of Omicron BA.1, BA.2, and BA.3
620 SARS-CoV-2 by 3 doses of BNT162b2 vaccine. *Nat. Commun*. 13(1):3602
- 621 Kurhade C, Zou J, Xia H, Liu M, Chang HC, et al. 2023. Low neutralization of SARS-CoV-2 Omicron
622 BA.2.75.2, BQ.1.1 and XBB.1 by parental mRNA vaccine or a BA.5 bivalent booster. *Nat. Med*. 29(2):344–
623 47
- 624 Lentini A, Pereira A, Winqvist O, Reinius B. 2022. Monitoring of the SARS-CoV-2 Omicron BA.1/BA.2
625 lineage transition in the Swedish population reveals increased viral RNA levels in BA.2 cases. *Med (N.*
626 *York, Ny)*. 3(9):636-643.e4

- 627 Li H. 2013. Aligning sequence reads, clone sequences and assembly contigs with BWA-MEM. arXiv
- 628 Ma KC, Shirk P, Lambrou AS, Hassell N, Zheng X, et al. 2023. Genomic Surveillance for SARS-CoV-2
629 Variants: Circulation of Omicron Lineages — United States, January 2022–May 2023. *Morb. Mortal. Wkly.*
630 *Rep.* 72(24):651–56
- 631 Malato J, Ribeiro RM, Fernandes E, Leite PP, Casaca P, et al. 2023. Stability of hybrid versus vaccine
632 immunity against BA.5 infection over 8 months. *Lancet Infect. Dis.* 23(2):148–50
- 633 Markov PV, Ghafari M, Beer M, Lythgoe K, Simmonds P, et al. 2023. The evolution of SARS-CoV-2. *Nat*
634 *Rev Microbiol.* 1–19
- 635 Meijers M, Ruchnewitz D, Eberhardt J, Łuksza M, Lässig M. 2023. Population immunity predicts
636 evolutionary trajectories of SARS-CoV-2. *Cell*
- 637 Muecksch F, Wang Z, Cho A, Gaebler C, Tanfous TB, et al. 2022. Increased memory B cell potency and
638 breadth after a SARS-CoV-2 mRNA boost. *Nature.* 1–7
- 639 Musalkova D, Piherova L, Kwasny O, Dindova Z, Stancik L, et al. 2023. Trends in SARS-CoV-2 cycle
640 threshold values in the Czech Republic from April 2020 to April 2022. *Sci. Rep.* 13(1):6156
- 641 Mykytyn AZ, Fouchier RA, Haagmans BL. 2023a. Antigenic evolution of SARS coronavirus 2. *Curr. Opin.*
642 *Viol.* 62:101349
- 643 Mykytyn AZ, Rosu ME, Kok A, Rissmann M, Amerongen G van, et al. 2023b. Antigenic mapping of
644 emerging SARS-CoV-2 omicron variants BM.1.1.1, BQ.1.1, and XBB.1. *Lancet Microbe.* 4(5):e294–95
- 645 Nouvellet P, Cori A, Garske T, Blake IM, Dorigatti I, et al. 2018. A simple approach to measure
646 transmissibility and forecast incidence. *Epidemics.* 22:29–35
- 647 O’Toole Á, Scher E, Underwood A, Jackson B, Hill V, et al. 2021. Assignment of Epidemiological Lineages
648 in an Emerging Pandemic Using the Pangolin Tool. *Virus Evol.* 7(2):veab064-
- 649 Park Y-J, Pinto D, Walls AC, Liu Z, Marco AD, et al. 2022. Imprinted antibody responses against SARS-
650 CoV-2 Omicron sublineages. *Science.* 378(6620):619–27
- 651 Petrone ME, Rothman JE, Breban MI, Ott IM, Russell A, et al. 2022. Combining genomic and
652 epidemiological data to compare the transmissibility of SARS-CoV-2 variants Alpha and Iota. *Commun*
653 *Biology.* 5(1):439
- 654 R Core Team (2021) R: A Language and Environment for Statistical Computing. R Foundation for Statistical
655 Computing, Vienna. www.R-project.org
- 656 Rambaut A, Loman N, Pybus O, Barclay W, Barrett J, et al. 2020. Preliminary genomic characterisation of
657 an emergent SARS-CoV-2 lineage in the UK defined by a novel set of spike mutations. virological.org
- 658 Rössler A, Netzl A, Knabl L, Schäfer H, Wilks SH, et al. 2022. BA.2 and BA.5 omicron differ
659 immunologically from both BA.1 omicron and pre-omicron variants. *Nat. Commun.* 13(1):7701
- 660 Schaefer-Babajew D, Wang Z, Muecksch F, Cho A, Loewe M, et al. 2022. Antibody feedback regulates
661 immune memory after SARS-CoV-2 mRNA vaccination. *Nature.* 1–3
- 662 Simon-Loriere E, Schwartz O. 2022. Towards SARS-CoV-2 serotypes? *Nat. Rev. Microbiol.* 20(4):187–88
- 663 Springer DN, Medits I, Weseslindtner L, Stiasny K, Aberle JH. 2023. SARS-CoV-2 neutralising antibody
664 response to bivalent booster after omicron infection. *Lancet Microbe*

- 665 Tan CW, Chia WN, Zhu F, Young BE, Chantasrisawad N, et al. 2022. SARS-CoV-2 Omicron variant
666 emerged under immune selection. *Nat. Microbiol.* 7(11):1756–61
- 667 Team C-19 F, Stein C, Nassereldine H, Sorensen RJD, Amlag JO, et al. 2023. Past SARS-CoV-2 infection
668 protection against re-infection: a systematic review and meta-analysis. *Lancet.* 401(10379):833–42
- 669 Tegally H, Moir M, Everatt J, Giovanetti M, Scheepers C, et al. 2022. Emergence of SARS-CoV-2 Omicron
670 lineages BA.4 and BA.5 in South Africa. *Nat. Med.* 28(9):1785–90
- 671 Tegally H, Wilkinson E, Giovanetti M, Iranzadeh A, Fonseca V, et al. 2021. Detection of a SARS-CoV-2
672 variant of concern in South Africa. *Nature.* 1–6
- 673 Tegally H, Wilkinson E, Tsui JL-H, Moir M, Martin D, et al. 2023. Dispersal Patterns and Influence of Air
674 Travel During the Global Expansion of SARS-CoV-2 Variants of Concern. *Cell*
- 675 Viana R, Moyo S, Amoako DG, Tegally H, Scheepers C, et al. 2022. Rapid epidemic expansion of the
676 SARS-CoV-2 Omicron variant in southern Africa. *Nature.* 1–10
- 677 Vogels CBF, Breban MI, Ott IM, Alpert T, Petrone ME, et al. 2021. Multiplex qPCR discriminates variants
678 of concern to enhance global surveillance of SARS-CoV-2. *Plos Biol.* 19(5):e3001236
- 679 WHO. 2021. COVID-19 Weekly Epidemiological Update.
- 680 Zhou J, Sukhova K, Peacock TP, McKay PF, Brown JC, et al. 2023. Omicron breakthrough infections in
681 vaccinated or previously infected hamsters. *Proc. Natl. Acad. Sci.* 120(45):e2308655120